19th Australasian Fluid Mechanics Conference
Melbourne, Australia
8-11 December 2014

Effect of Interfacial Tension and Electric Field on Charge Separation Dynamics Inside Stable and Unstable Microdrops

R. Pillai[1], J. D. Berry[2], D. J. E. Harvie[1] and M. R. Davidson[1]

[1]Department of Chemical and Biomolecular Engineering
The University of Melbourne, Melbourne, Victoria 3000, Australia

[2]CSIRO Mineral Resources
Clayton, Victoria 3168, Australia

Abstract

In this paper, charge separation behaviour inside a microscale drop of water suspended in oil is studied using a novel electrokinetic model [1], which allows for conduction, convection and diffusion of ions inside the drop. The interfacial tension and electric field are varied and its effects on charge separation studied. It is shown that the concentration of charge varies inside the drop as ions redistribute in response to electrical forces. The charge separation measured at the centre is similar for the stable and unstable cases considered. For the unstable drops, a significant proportion of the charge collects near the interface of the drop and is ejected as the drop breaks.

Introduction

Droplet microfluidics has many uses in chemical and biological research because each drop can be treated as an isolated microreactor in large scale batch experiments enabling greater throughput and scalability [2]. Microfluidic droplet-based Lab-on-Chip (LoC) devices require the ability to generate and manipulate discrete droplets, using immiscible phases, in microscale sized channels. When the drop or the continuous phase in the LoC is an electrolyte, the necessary drop manipulation can be performed by utilizing an external electric field which selectively acts on the conducting phase. Electrokinetic techniques have been widely employed in droplet based microfluidics for applications including forming, sorting, coalescing and breaking up droplets [3, 4, 5, 6].

Though the problem of electrically induced deformation of a conducting drop suspended in an immiscible continuous phase has only recently gained prominence in microfluidics, it has been a classic problem for macroscale flows [7]. It is therefore not surprising that the electric field models developed to predict macroscale drop deformation have been adapted for microscale flows. For conducting drops, the existing numerical models do not account for the dynamic ion behaviour inside the drop and make various simplifying assumptions regarding the location of ions inside the drop. The most common model is called the leaky dielectric model which assumes that the free charge is confined to the interface. This assumption, which implies that the electrical double layer (EDL) is infinitely thin, is shown to be invalid for large deformations even for macroscale flows [8]. For microfluidic flows, the thickness of the EDL layer is not insignificant compared to drop diameter and interfacial effects are of greater importance [9]. It is therefore more appropriate to use an electrokinetic model, which allows for diffuse regions of charge to form and be transported in response to the external electric field, to study microfluidic drops.

The goal in this paper is to investigate the deformation and breakup behaviour of an initially spherical, conducting microfluidic drop of water suspended in a non conducting oil phase, and acted on by an external field. We study the effects of different electric field-interface tension combinations which are the two main forces involved in drop deformation. Interfacial tension variations achieved through the use of surfactants [10] have been shown to affect drop deformation dynamics and hence the study of water-oil systems with varying interfacial tension has practical applications. In particular, we study the charge separation behaviour for both stable and unstable drops and contrast them.

Numerical Model

Berry et al. [1] formulated a Combined Level Set Volume of Fluid (CLSVoF) based electrokinetic model for liquid/liquid interfaces which allows for the coupled calculation of convective, conductive and diffusive ion transport, the electrical potential distribution, and the flow dynamics of the liquid phases. This model has been shown to predict different dynamic drop behaviours dependent on the conductivity of the drop and the strength of the electrical field which cannot be captured by simplified electric field models [11].

An axisymmetric drop of radius R is considered, with permittivity ε_d, density ρ_d and viscosity μ_d (Corresponding continuous phase properties are represented using the subscript 'c' like ε_c, ρ_c and μ_c). The drop contains symmetric anions and cations (with concentrations n_+ and n_-, respectively) with valencies $z_+ = z_- = z$, and diffusivities $\alpha_+ = \alpha_- = \alpha$. The initial drop ion concentration is given by the geometric mean of the species ion concentrations ($n_0 = \sqrt{n_+ n_-}$). The drop is suspended in a dielectric medium of permittivity ε_c. The interface between the drop and continuous phase is assumed to have a constant interfacial tension γ and zero interface charge. The algorithm of Berry et al. [1] has recently been extended to include interface charge [12] and will be used in future work.

Governing Equations

The characteristic length scale is R, permittivity scale is ε_d, ion scale is n_0, velocity scale is $V_{\text{ref}} = \gamma/\mu_d$ and the electric field scale is $E_{\text{ref}} = kT/zeR$.

All physical variables are non-dimensionalized to characterize the system,

$$x = \frac{x^*}{R};\ V = \frac{v^*}{V_{\text{ref}}};\ \varepsilon = \frac{\varepsilon^*}{\varepsilon_d};\rho = \frac{\rho^*}{\rho_d};\mu = \frac{\mu^*}{\mu_d};\ n_\pm = \frac{{n_\pm}^*}{n_0};\ E = \frac{E^*}{E_{\text{ref}}}$$

The relevant non-dimensional numbers are:

$$\text{Re} = \frac{\rho_d V_{\text{ref}} R}{\mu_d};\ \text{We} = \frac{\rho_d V_{\text{ref}}^2 R}{\gamma};\ \text{Pe} = \frac{V_{\text{ref}} R}{\alpha};\ \text{B} = \frac{\rho_d k^2 T^2 \varepsilon_0 \varepsilon_d}{2 z^2 e^2 \mu_d^2}$$

where Re is the Reynolds number, We the Weber number, Pe the Péclet number and B is a parameter that is fixed for a given liquid, in this case water, at a fixed temperature. The thickness of

the diffuse layer is characterized by the inverse nondimensional Debye length, or K_d, given by

$$K_\mathrm{d} = \sqrt{\frac{2z^2e^2n_0R^2}{\varepsilon_0\varepsilon_\mathrm{d}kT}}$$

Here e, T and k are the electron charge, temperature and Boltzmann constant respectively. In the problem studied here, there is no charged surface as the drop interface is uncharged. However, in the influence of the external field, the ions inside the drop redistribute in a manner analogous to ions in a diffuse layer adjacent to a charged surface.

The dimensionless equations governing the electrical field, the flow and ion concentration are:

$$\nabla\cdot(\varepsilon\boldsymbol{E}) = \frac{1}{2}K_\mathrm{d}^2 q \quad (1)$$

$$\nabla\cdot\boldsymbol{u} = 0 \quad (2)$$

$$\frac{\partial\rho\boldsymbol{u}}{\partial t} + \nabla\cdot(\rho\boldsymbol{u}\boldsymbol{u}) = -\nabla p + \frac{1}{\mathrm{Re}}\nabla\cdot\boldsymbol{\tau_V} + \frac{1}{\mathrm{We}}\boldsymbol{F}_\mathrm{S} + \frac{2\mathrm{B}}{\mathrm{Re}^2}\boldsymbol{F}_\mathrm{E} \quad (3)$$

$$\frac{\partial cn_\pm}{\partial t} + \nabla\cdot(\boldsymbol{u}cn_\pm) = \frac{1}{\mathrm{Pe}}\nabla\cdot[c\nabla n_\pm \mp cn_\pm\boldsymbol{E}] \quad (4)$$

$$\frac{\partial c}{\partial t} + \nabla\cdot(c\boldsymbol{u}) = 0 \quad (5)$$

$\boldsymbol{\tau_V}$ and p are the viscous stress tensor and pressure respectively. Equation 1 is the Poisson equation for the electric potential where q is the dimensionless drop charge density ($q = n_+ - n_-$). Equation 5 is the transport equation for the disperse volume fraction c. In equation 3, $\boldsymbol{F}_\mathrm{S}$ is the force due to the interfacial tension and $\boldsymbol{F}_\mathrm{E}$ is the electrical force term represented by the divergence of the Maxwell stress tensor.

$$\boldsymbol{F}_\mathrm{E} = \nabla\cdot\boldsymbol{\tau_M} = \nabla\cdot[\varepsilon\boldsymbol{E}\boldsymbol{E} - \frac{1}{2}\varepsilon(\boldsymbol{E}\cdot\boldsymbol{E})\boldsymbol{I}]$$

Problem Setup

The drop is assumed to be spherical initially and is located at the centre of the domain with vertical dimensions of $30R$ and width $4R$. A uniform external field E_o^* is imposed along the Z axial direction of the drop, thus deforming it. An important dimensionless parameter used to represent the ratio of electric and interfacial tension forces is the Electric Capillary number ($\mathrm{Ca_E}$)

$$\mathrm{Ca_E} = \frac{\varepsilon_0\varepsilon_\mathrm{d}R}{\gamma}E_o^{*2}$$

Using the scaling described above, this is recast as

$$\mathrm{Ca_E} = 2\,\mathrm{B}\,\mathrm{Oh}^2 E_o^2 \quad (6)$$

where Oh is the Ohnesorge number

$$\mathrm{Oh} = \frac{\sqrt{\mathrm{We}}}{\mathrm{Re}} = \frac{\mu_\mathrm{d}}{\sqrt{\rho_\mathrm{d}\gamma R}} \quad (7)$$

Results and Discussion

Fixing $\mathrm{Ca_E}$ while varying Oh physically corresponds to varying both the electric field (E_o^*) and interfacial tension (γ) (assuming that other physical parameters are held constant). The initial ion concentration in the drop is fixed for all cases as K_d is constant.

Results are presented here for a water drop suspended in oil, a system commonly found in microfluidic LoC devices. The

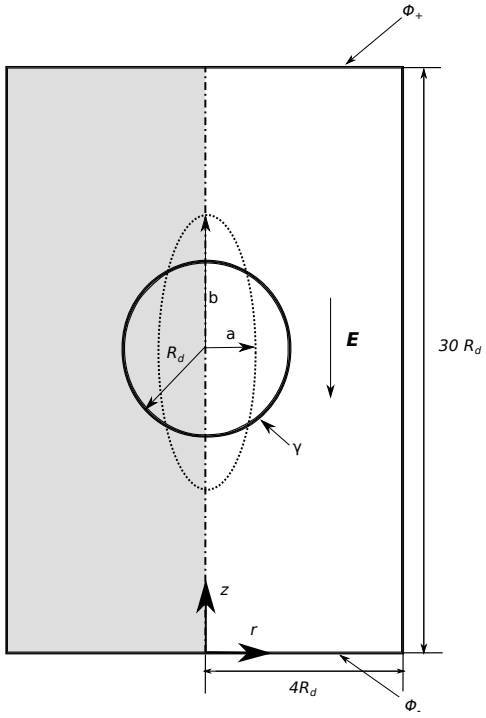

Figure 1: Schematic of problem

Parameter	Value
Drop Radius, R	10 μm
Drop Permittivity, ε_d	80×8.885 pF/m
Oil Permittivity, ε_c	1.6×8.885 pF/m
Drop Viscosity, μ_d	10^{-3} Pa.s
Drop Density, ρ_d	10^3 kg/m^3
Electric Capillary Number, $\mathrm{Ca_E}$	0.26
Inverse Debye Length, K_d	3

Table 1: Parameters for the cases considered

parameters for which are given in Table 1. To simplify the problem, the drop and continuous phase are assumed to have equal viscosity and density. Oils with the same viscosity as water are common (see NN1 and NN2 from Ha et al. [13]), and density variations have been shown to have negligible impact on drop deformation. The permittivity ratio $Q = \varepsilon_\mathrm{d}/\varepsilon_\mathrm{c} = 50$. Three values of interfacial tension are used, $\gamma = 10^{-2}$, 10^{-3} and 10^{-4} N/m which correspond to $\mathrm{Oh}^2 = 10^{-1}$, 10^0 and 10^1 respectively. As $\mathrm{Ca_E}$ is constant, the external electric field varies inversely with Oh as seen in equation 6.

Deformation behaviour

In the absence of ions, the right hand side of equation 1 is zero. The electrical force then simplifies to

$$\boldsymbol{F}_\mathrm{E} = -\boldsymbol{E}\cdot\boldsymbol{E}\nabla\varepsilon \quad (8)$$

The only force deforming the drop is due to the electric field acting on the permittivity difference at the drop interface. When ions are present, regions of charge can form and there is a second force component deforming the drop, along with the permittivity force, due to the charge called the charge force [11]. The ions are initially distributed in equal numbers to ensure electrical neutrality, thus zero charge, everywhere inside the

drop. When the electric field is first applied, equal but opposite electric conductive fluxes are imparted to anions and cations. This results in cations travelling towards one end of the drop in the direction of the external electric field. The anions are conducted in the opposite direction. Regions of charge are formed when either ion species gets depleted relative to the other. This process begins at the tips as the ions conduct away towards the opposite tip. The electric field acts on the charge developed, creating the charge force deforming the drop. As a result of the permittivity and charge electrical forces, the drop elongates along the direction of the electrical field until arrested by the opposing interfacial tension if the drop is stable. If the electric field is sufficiently high or the interfacial tension is sufficiently low, the electrical deforming forces overcome the resisting interfacial tension forces and the drop breaks up.

The deformation of a drop is normalized by the deformation parameter D, where a and b are the length of the axes of the drop perpendicular and parallel to the electrical field respectively.

$$D = \frac{b-a}{b+a} \tag{9}$$

Figure 2 traces the deformation with time for the three cases outlined earlier. The drop deformation behaviour is faster the lower the Oh (higher electric field and interfacial tension). The plotting continues until the drop has reached stability or has broken up. The behaviour of the $\mathrm{Oh}^2 = 10^0$ and $\mathrm{Oh}^2 = 10^1$ cases appear largely similar, with a gradual increase preceding a steep rise at the tail end of the curve. This deformation behaviour is associated with the formation of lobes at both ends of the drop. These lobes then accelerate and pinch-off from the main drop to form droplets as the main drop breaks up [11]. However the deformation curve for $\mathrm{Oh}^2 = 10^{-1}$ does not display similar acceleration and instead stabilizes to a constant value. The embedded final drop shapes show the drop has attained a stable shape. The other two cases, in contrast, achieve breakup. Among the cases that have broken up it can be seen that the droplet breaking off in the $\mathrm{Oh}^2 = 10^1$ case is slightly flatter than that ejected by the $\mathrm{Oh}^2 = 10^0$ case. This could be because the higher interfacial tension for the $\mathrm{Oh} = 10^0$ case helps the ejected droplet retain its spherical shape.

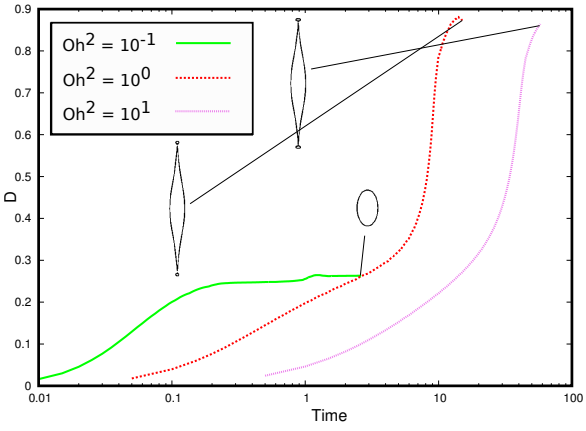

Figure 2: Comparison of deformation curves for $\mathrm{Oh}^2 = 10^{-1}$, 10^0 and 10^1. Embedded images show final drop shape ($\mathrm{Oh}^2 = 10^{-1}$) and shapes at breakup after which data is no longer plotted ($\mathrm{Oh}^2 = 10^0$, 10^1) respectively

Stable and Unstable Drops

It has been shown that drops which do not contain ions cannot breakup via ejection of droplets at both ends [11]. The destabilization and breakup of the drop in this manner requires the presence of tangential stresses created by the moving charge inside the drop. As figure 2 shows, for identical ion concentrations, drops can either be stable or unstable depending on the relative strength of the electric field and interface tension. This indicates that the charge separation dynamics inside the drop is affected by the choice of Oh. To investigate this further, the variation of the percentage of ions of each species in one half of the drop with time is plotted in figure 3. This can be treated as an approximation of the charge separation process inside the drop. The fact that the charge behaviour is symmetrical across the horizontal centerline makes the approximation possible. Since the top half of the drop is considered, the anions conduct into the half and cations conduct out of the half. Consequently, the percentage of anions increases while that of cations decreases and this is true for all cases considered.

However, the charge separation rate, measured at the centerline, appears to be qualitatively similar for all three values of Oh^2. This is despite the fact that $\mathrm{Oh}^2 = 10^{-1}$ case is stable while $\mathrm{Oh}^2 = 10^0, 10^1$ cases are unstable and charge separation is the driver for the electrical force acting at the drop tips and resulting in drop breakup.

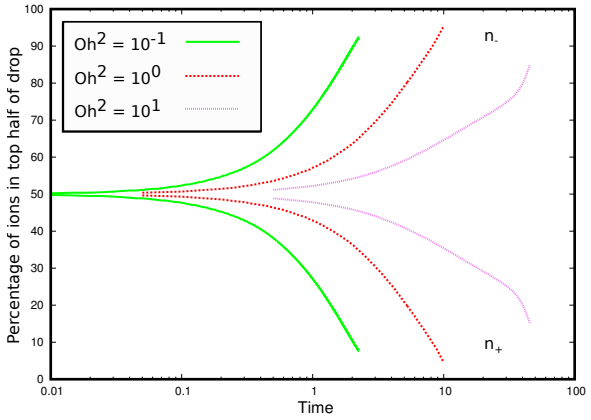

Figure 3: The percentage of cations (bottom group) and anions (top group) in top half of the drop for $\mathrm{Oh}^2 = 10^{-1}$, 10^0 and 10^1

It can also be seen that the rate of charge separation does not appear to be decreasing with time. No equilibrium appears to have been reached between the conductive, convective and diffusive fluxes governing ion transport inside the drop for the cases considered. Note that the drop dimensions for $\mathrm{Oh}^2 = 10^{-1}$ have stabilized but conduction of charge across the centerline continues.

The fact that the $\mathrm{Oh}^2 = 10^{-1}$ case is stable implies that the charge separation isn't sufficient to destabilize drops for the lowest value of Oh^2 considered. To probe the dynamics of the charge separation further, the mean ion location in the drop along the Z axis is plotted for all three cases considered. In order to disregard the temporal differences in deformation behaviour between the cases, the ion location is plotted with D. In this plot 1 is the centre of the domain and drop while 0 and 2 are the bottom and top of the domain respectively. The location of the drop tips is also included and the variation of drop tip with D is the same for all drops. Here the differences between the stable and unstable cases become clearer. First, the two unstable drops have similar profiles. The section between $D = 0.1$ and $D = 1$ is where some differences appear as the drops transition from well under the stability limit ($D = 0.1$) to unstable ($D \to 1$). It can be seen that the mean ion location shows the

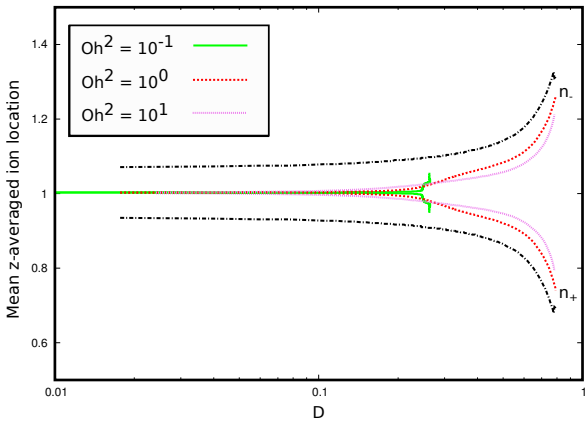

Figure 4: Comparison of mean ion location curves for cations (bottom group) and anions (top group) for $\mathrm{Oh}^2 = 10^{-1}$, 10^0 and 10^1. The black lines show the location of the drop tips.

greatest variation in this region for both the unstable cases. The mean location is affected by the motion of regions of drop as it breaks up, implying that a significant amount of the charge separated is concentrated in the lobe that accelerates and breaks away from the main drop. In contrast, the mean location of the ions for $\mathrm{Oh} = 10^{-1}$ is much closer to the centre of the domain. This shows that even though the charge separation when measured at the centre of the drop appears to be similar for stable and unstable drops, the location of the ions is different because in unstable drops, the bulk of the charge destabilizes the drop tip and breaks off from the main drop.

The mean ion location for the $\mathrm{Oh}^2 = 10^0$ case is further from the centre of the domain than the $\mathrm{Oh}^2 = 10^1$ case. This implies that a greater volume of charge separation is required to achieve the same deformation value for the $\mathrm{Oh}^2 = 10^1$ case, possibly because of the higher interfacial tension resisting the formation of a lobe on the surface of the drop. This is consistent with the ejection of the slightly larger droplet for the $\mathrm{Oh}^2 = 10^1$ case at breakup in fig 2.

The mean ion curve for the stable case has interesting features. The deformation of the drop attains a maximum value of $D = 0.263$ and hence the curve does not extend to the right end of the plot. However, this does not imply that the charge separation inside the drop has achieved a steady equilibrium. As seen here, despite the dimensions of the drop being stable, the mean ion location continues to move steadily away from the centre as indicated by the small vertical lines for fixed D. This implies that the process of conduction of ions followed by accumulation of charge at the ends of the drop has not ceased consistent with the charge separation results. Note that the total force deforming the drop appears to be stable because the drop dimensions appear to have attained steady state values. This aspect of stable drop dynamics wherein the electric force associated with charge is increasing but total electric force is constant, requires further study. It can be concluded that for $\mathrm{Oh} = 10^{-1}$, the timescale for charge separation is significantly greater than the timescale for drop deformation. This results in the drop stabilizing before the charge dynamics inside the drop have reached an equilibrium. It therefore cannot be stated with complete certainty that the drop is stable at all, as ongoing charge dynamics inside the drop can possibly destabilize it at a given future time.

Conclusions

Results are presented for charge separation behaviour inside a microscale drop of water suspended in oil, studied using a novel electrokinetic model [1]. It is shown that the concentration of charge varies inside the drop in the presence of an external electric field, as ions redistribute in response to electrical forces. The stability of the drop for the cases considered is shown to be largely independent of the number of cations and anions in each half of the drop. Instead, it is the location of the ions that differentiates stable from unstable drops. Also for the stable case considered here, the accumulation of charge on the drop interface continues after the dimensions of the drop have apparently stabilized. The effect of the charge separation on the total force deforming the drop warrants further investigation.

References

[1] Berry, J.D., Davidson, M.R. and Harvie, D.J.E., A multiphase electrokinetic flow model for electrolytes with liquid/liquid interfaces. *Journal of Computational Physics* **251**, 2013

[2] Theberge, A.B., Courtois, F., Schaerli, Y., Fischlechner, M., Abell, C., Hollfelder, F. and Huck, W.T.S., Microdroplets in microfluidics: an evolving platform for discoveries in chemistry and biology. *Angewandte Chemie*, **49(34)** 2010.

[3] Park, J., High-resolution electrohydrodynamic jet printing. *Nature Materials*, **6(10)**, 2007.

[4] Ahn, K., Kerbage, C., Hunt, T.P. Westervelt, R.M. and Link, D.R., Dielectrophoretic manipulation of drops for high-speed microfluidic sorting devices. *Applied Physics Letters*, **88** (2):024104, 2006.

[5] Zagnoni, M., Le Lain, G. and Cooper, J.M., Electrocoalescence mechanisms of microdroplets using localized electric fields in microfluidic channels. *Langmuir*, **26(18)**, 2010.

[6] Link, D., Anna, S., Weitz, D. and Stone, H., Geometrically mediated breakup of drops in microfluidic devices. *Physical Review Letters*, **92(5)**:054503, 2004.

[7] Rayleigh, L., On the equilibrium of liquid conducting masses charged with electricity. *Philosophical Magazine Series 5*, **14**, 1882

[8] Torza, S. Cox, R.G. and Mason, S.G., Electrohydrodynamic deformation and burst of liquid drops. *Philosophical Transactions of the Royal Society*, **269(1198)**, 1971.

[9] Squires, T. M. and Quake, S.R., Microfluidics: nanoliter scale. *Reviews of Modern Physics*, **77**, 2005.

[10] Teigen, K. and Munkejord, S.T., Influence of surfactant on drop deformation in an electric field. *Physics of Fluids* **11**, 2010

[11] Pillai, R., Berry, J.D., Harvie, D.J.E. and Davidson, M.R., Electrokinetic effects on drop dynamics when subjected to a steady electric field *(In preparation)* 2014

[12] Davidson, M. R., Berry, J.D. and Harvie, D.J.E., Numerical simulation of the deformation of charged drops of electrolyte *Advances in Fluid Mechanics X*, **82**, WIT Press, 2014

[13] Ha, J. and Yang, S., Deformation and breakup of Newtonian and non-Newtonian conducting drops in an electric field. *Journal of Fluid Mechanics*, **405**, 2000.